HTML ABSTRACT + LINKS

High-speed 1.3 μm tunnel injection quantum-dot lasers

Z. Mi, P. Bhattacharya,[a] and S. Fathpour
Solid State Electronics Laboratory, Department of Electrical Engineering and Computer Science, The University of Michigan, Ann Arbor, Michigan 48109-2122

(Received 10 January 2005; accepted 21 February 2005; published online 5 April 2005)

1.3 μm tunnel injection quantum-dot lasers are demonstrated. The laser heterostructures are grown by molecular-beam epitaxy. The InAs self-organized quantum dots are p doped to optimize the gain. The lasers are characterized by $J_{\mathrm{th}}=180$ A/cm^2, $T_0=\infty$, $dg/dn \approx 1\times 10^{-14}$ cm^2, $f_{-3\mathrm{dB}}=11$ GHz, chirp of 0.1 Å, and zero α parameter. © *2005 American Institute of Physics*. [DOI: 10.1063/1.1899230]

Since the first demonstration of 1.3 μm quantum-dot (QD) lasers,[1] many groups have reported the characteristics of these devices.[2–4] However, the achievement of large modulation bandwidth (>10 GHz), accompanied by low chirp and α parameter, has been elusive. A small-signal modulation bandwidth of 12 GHz was recently reported for an InGaAs QD laser in which the quantum dots were grown on an InGaP buffer layer.[5] However, no data on chirp and α parameter were reported by these authors. In order to extract enhanced performance from these devices, it is first important to understand some fundamental limitation arising from the unique hot carrier dynamics in quantum dots. It is now well recognized that the wetting layer, formed during Stranski-Krastanow growth of the QD islands, has a major influence on QD laser performance. The localized QD states and the two-dimensional wetting layer/barrier states of the dot heterostructures form an electronically coupled system.[6] Since the number of wetting layer/barrier states is much larger than the number of available dot states at room temperature, injected electrons predominantly reside in the wetting layer/barrier states and the system cannot be described by equilibrium quasi-Fermi statistics.

Tunnel injection has been used very effectively in suppressing hot-carrier related problems in quantum-well lasers[7] and in achieving high-speed modulation of 1 μm QD lasers.[7,8] In this technique cold carriers (electrons) are injected by tunneling in the QD lasing states and thus they do not heat other carriers or phonons as much, resulting in reduced carrier leakage from the active region and recombination in the cladding layers. As a result, the characteristic temperature T_0 is enhanced and the differential gain dg/dn increases substantially, leading to enhanced modulation bandwidth
(24.5 GHz in 1.1 μm QD lasers) and reduced threshold current. The technique of acceptor (p) doping of the quantum dots has also been proposed as a means of improving QD laser performance.[9,10] Acceptor doping ensures that the hole ground states are filled, thereby substantially increasing the gain and also the differential gain by a small amount. In this letter we report the small-signal modulation characteristics of high-performance single-mode InAs QD lasers in which tunnel injection and p doping are *both* incorporated. The lasers demonstrate a small-signal −3 dB bandwidth of 11 GHz, together with zero α-parameter values and negligible chirp.

[a]Electronic mail: pkb@eecs.umich.edu

The band diagram in the active region of the separate confinement heterostructure (SCH) QD tunnel injection lasers is schematically illustrated in Fig. 1(a). The inset shows one period of the injector layer, tunnel barrier, and quantum dot. It is important to note that in our heterostructure design, the electrons from the injector are made to tunnel at an energy close to the dot first excited states and separated from them by the energy of a LO phonon. We have determined, theoretically[11] and experimentally by pump-probe differential transmission spectroscopy measurements,[12] that the relaxation time from the dot excited states to the ground state is very small, ~1–2 ps, if the excited states are filled with

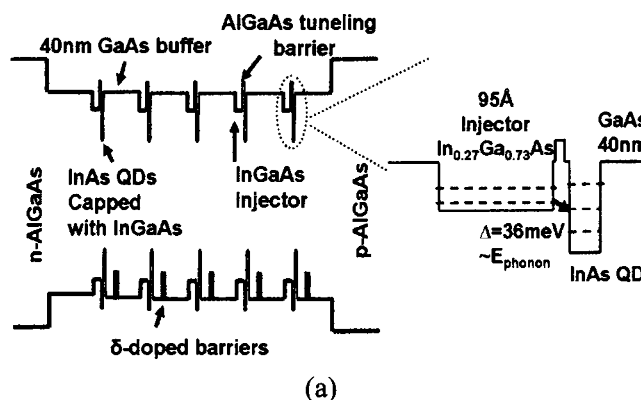

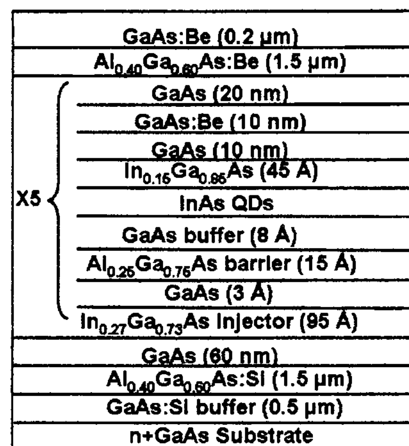

FIG. 1. (a) Schematic band diagram of the 1.3 μm p-doped tunnel injection QD laser active region and (b) laser heterostructure grown by molecular-beam epitaxy.

 © 2005 American Institute of Physics

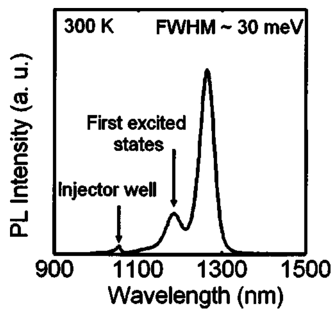

FIG. 2. Room-temperature PL spectra of the 1.3 μm p-doped tunnel injection QD laser heterostructure.

electrons. This is due to very efficient electron-hole and electron-electron scattering in the dots under large injection (lasing) conditions. The complete laser heterostructure, shown in Fig. 1(b), was grown by molecular-beam epitaxy on (001) n^+-GaAs substrate. P-type modulation doping of the quantum dots in each of the five layers is done with beryllium. The peaks corresponding to emission from the QD and injector layer in the room-temperature photoluminescence (PL) spectra are carefully tuned such that the ground state in the injector quantum well is one LO phonon energy above the first excited state energies in the QD. The laser heterostructures exhibit strong luminescence at room temperature, as shown in Fig. 2, where the different peaks are identified. Laser heterostructures in which the composition of the tunnel barrier was changed to $Al_{0.40}Ga_{0.60}As$ and $Al_{0.10}Ga_{0.90}As$, all else remaining the same, were also grown under identical conditions. Both mesa-shaped broad area lasers of dimensions $(20-200\ \mu m)\times(500-2000\ \mu m)$ and single-mode ridge waveguide lasers of 3 μm ridge width and varying length were fabricated by standard photolithography, wet and dry etching, and contact metallization techniques. In this letter, we will describe the properties of the lasers with $Al_{0.25}Ga_{0.75}As$ tunnel injection barriers, as shown in Fig. 1(b).

Both cavity length-dependent and temperature-dependent light-current (LI) measurements were performed under a quasi-cw condition (10% duty cycle). The devices demonstrate low threshold current (180 A/cm^2) and reasonable output slope efficiency (0.39 W/A) for an 800 $\times 5\ \mu m^2$ device with a high reflectivity (HR) coating (95%) on one facet. The characteristics are shown in Fig. 3(a), wherein the inset shows the spectral output at threshold. From the cavity-length-dependent measurements, we derive values of the cavity loss γ and internal quantum efficiency η_i equal to 6.3 cm^{-1} and 71%, respectively. The variation of threshold current with temperature, measured in 400 $\times 5\ \mu m^2$ devices with HR coating on both facets, is depicted in Fig. 3(b). Temperature-independent threshold current ($T_0 = \infty$) is observed in the temperature range 5–70 °C. Detailed analysis[13] provides evidence that the temperature dependence of Auger recombination in the quantum dots[14] explains this behavior. Also shown in Fig. 3(b) is the temperature dependence of the output slope efficiency.

Small-signal modulation measurements were made to determine the frequency response of the lasers. The devices were biased with a pulse generator and rf sweep oscillator through a bias T. The laser output was detected with a 40 GHz InGaAs detector, the output of which was amplified by a low-noise amplifier, before being displayed on a spec-

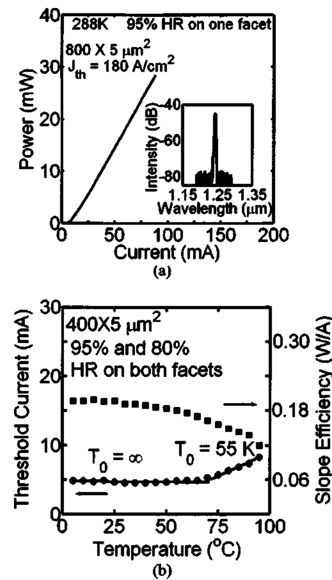

FIG. 3. Characteristics of p-doped 1.3 μm tunnel injection QD lasers: (a) light-current with output spectrum (inset), and (b) variation of threshold current and output slope efficiency with temperature.

trum analyzer. The modulation response characteristics of a single-mode $400\times 3\ \mu m^2$ device are illustrated in Fig. 4(a). A maximum modulation bandwidth of 11 GHz is measured. From a plot of the resonance frequency f_r versus the square root of the injection current, $(I-I_{th})^{1/2}$, a modulation efficiency of 1.07 GHz/mA$^{1/2}$ and a differential gain $dg/dn = 8\times 10^{-15}$ cm^2 are derived. The latter is in good agreement with the value of $dg/dn = 9.8\times 10^{-15}$ cm^2 derived from cavity-length-dependent measurements just described.

For comparison, it is worth mentioning that the maximum 3 dB bandwidths of the lasers with $Al_{0.40}Ga_{0.60}As$ and $Al_{0.10}Ga_{0.90}As$ tunnel barriers are 9 and 7 GHz, respectively. The measured threshold currents are similar to the device described earlier. It is evident that the laser with the $Al_{0.10}Ga_{0.90}As$ barrier behaves more like a conventional SCH quantum-dot laser. In the laser with the $Al_{0.40}Ga_{0.60}As$ barrier, the slightly lower bandwidth may be due to inefficient carrier transport to all the dot layers, resulting in gain compression at the lasing energy. The maximum measured 3 dB bandwidth of 11 GHz is substantially lower than 24.5 GHz measured in 1.1 μm p-doped tunnel injection lasers. The gain in the active region is proportional to the dot density (fill factor) and inversely proportional to the dot size and transition (PL) linewidth. The 1.3 μm quantum dots have larger dot size and smaller fill factor, resulting in devices with lower gain and saturation gain per dot layer ($\sim$10 cm^{-1}) compared to 1.1 μm QD lasers ($\sim$15 cm^{-1}). More important, the measured differential gain is lower in the 1.3 μm laser (8×10^{-15} cm^2) compared to that in the 1.1 μm laser (3×10^{-14} cm^2). Since the resonance frequency is proportional to the square root of the differential gain, in very approximate terms, a factor of 2 reduction in the bandwidth is expected. This is in agreement with our results. The measured bandwidth of 12 GHz in the 1.3 μm device by Kim *et al.*[5] is within the limits of experimental error. Therefore, it appears that the bandwidth of the 1.3 μm devices will be lower than the 1.0 or 1.1 μm devices.

The linewidth enhancement factors (α parameters) as a function of frequency were obtained by measuring the sub-

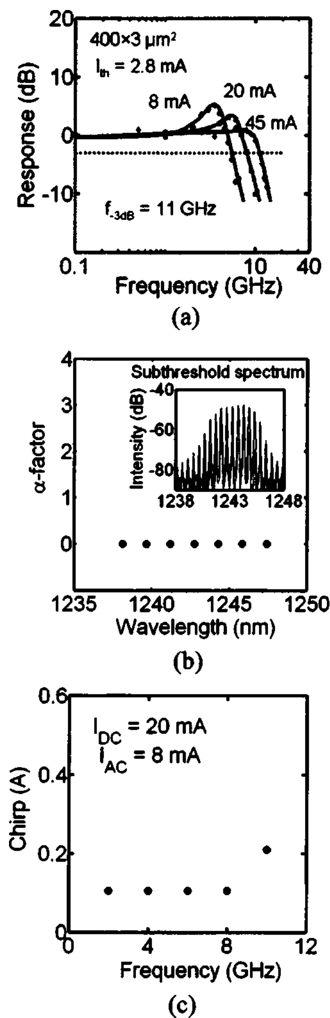

FIG. 4. (a) Small-signal modulation response, (b) linewidth enhancement factor with subthreshold spectrum (inset), and (c) chirp as a function of frequency.

threshold emission spectra of the single-mode tunnel injection ridge waveguide lasers and by calculating the Fabry-Pérot mode peak-to-valley ratios and shifts between two different pulsed bias currents. Shown in Fig. 4(b) is the wavelength (frequency) dependence of the linewidth enhancement factor. The values of the α parameters are essentially zero, since no shift in the Fabry-Pérot modes were detectable. There is direct evidence that the α parameters measured with other techniques[15] with the device operating beyond threshold, such as the injection locking technique, are in excellent agreement with the α parameters obtained by the subthreshold Hakki-Paoli measurements. Therefore, it is reasonable to conclude that the α parameters in the QD lasers are zero or very close to it.

The chirp in a semiconductor laser is directly proportional to the α parameters, since it is also related to the modulation of the refractive index of the gain region by the injected charge. We have measured the chirp in the QD lasers during small-signal modulation by measuring the broadening of a single longitudinal mode using an optical spectrum analyzer. The sinusoidal modulation current was superimposed on the pulsed dc bias current above threshold. The envelope of the dynamic shift in the wavelength was recorded and the difference between the half-width of the observed envelope with and without modulation was used to evaluate the chirp. The measurements were done as a function of the frequency and amplitude (peak-to-peak value) of the modulating current. Shown in Fig. 4(c) is the measured chirp as a function of the modulation frequency. As expected, the chirp is very low. The low values of α parameter and chirp also confirm the reduction in hot carrier density in the active volume of the QD lasers.

The work is being supported by the Army Research Office under Grant W911NF-04-1-0229 and by the Center for Optoelectronic Nanostructures Technologies (CONSRT), a DARPA UPR Award, under Contract No. HR0011–04–1–0040.

[1] D. L. Huffaker, G. Park, Z. Zou, O. B. Shchekin, and D. G. Deppe, Appl. Phys. Lett. **73**, 2564 (1998).
[2] S. Mukai, N. Ohtsuka, H. Shoji, M. Sugawara, N. Yokoyama, and H. Ishikawa, IEEE Photonics Technol. Lett. **11**, 1205 (1999).
[3] L. F. Lester, A. Stintz, H. Li, T. C. Newell, E. A. Pease, B. A. Fuchs, and K. J. Malloy, IEEE Photonics Technol. Lett. **11**, 931 (1999).
[4] A. E. Zhukov, A. R. Kovsh, V. M. Ustinov, Y. M. Sherynyakov, S. S. Mikhrin, N. A. Maleev, E. Y. Kondrat'eva, D. A. Livshits, M. V. Maximov, B. V. Volovik, D. A. Bedarev, Y. G. Musikhin, N. N. Ledentsov, P. S. Kop'ev, Z. I. Alferov, and D. Bimberg, IEEE Photonics Technol. Lett. **11**, 1345 (1999).
[5] S. M. Kim, Y. Wang, M. Keever, and J. S. Harris, IEEE Photonics Technol. Lett. **16**, 377 (2004).
[6] D. R. Matthews, H. D. Summers, P. M. Smowton, and M. Hopkinson, Appl. Phys. Lett. **81**, 4904 (2002).
[7] P. Bhattacharya, J. Singh, H. Yoon, X. Zhang, A. Gutierrez-Aitken, and L. Yam, IEEE J. Quantum Electron. **32**, 1620 (1996).
[8] P. Bhattacharya, S. Ghosh, S. Pradhan, J. Singh, Z.-K. Wu, J. Urayama, K. Kim, and T. B. Norris, IEEE J. Quantum Electron. **39**, 952 (2003).
[9] Y. Miyamoto, Y. Miyake, M. Asada, and Y. Suematsu, IEEE J. Quantum Electron. **25**, 2001 (1989).
[10] D. G. Deppe, H. Huang, and O. B. Shchekin, IEEE J. Quantum Electron. **38**, 1587 (2002).
[11] P. Bhattacharya, K. K. Kamath, J. Singh, D. Klotzkin, J. Phillips, H.-T. Jiang, N. Chervela, T. B. Norris, T. Sosnowski, J. Laskar, and R. Murty, IEEE Trans. Electron Devices **46**, 871 (1999).
[12] K. Kim, J. Urayama, T. B. Norris, J. Singh, J. Phillips, and P. Bhattacharya, Appl. Phys. Lett. **81**, 670 (2002).
[13] S. Fathpour, Z. Mi, S. Chakrabarti, P. Bhattacharya, A. R. Kovsh, S. S. Mikhrin, I. L. Krestnikov, A. V. Kozhukhov, and N. N. Ledentsov, Appl. Phys. Lett. **85**, 5164 (2004).
[14] S. Ghosh, P. Bhattacharya, E. Stoner, J. Singh, H. Jiang, S. Nuttinck, and J. Laskar, Appl. Phys. Lett. **79**, 722 (2001).
[15] G. Liu, X. Jin, and S. L. Chuang, IEEE Photonics Technol. Lett. **13**, 430 (2001).